Gain and current-density calculation in IV–VI quantum well lasers

M. F. Khodr and P. J. McCann
School of Electrical Engineering and Laboratory for Electronic Properties of Materials, University of Oklahoma, Norman, Oklahoma 73019

B. A. Mason
Department of Physics and Astronomy and Laboratory for Electronic Properties of Materials, University of Oklahoma, Norman, Oklahoma 73019

(Received 17 October 1994; accepted for publication 28 January 1995)

In this work, a theoretical model is used to study the gain versus current-density relationship for IV–VI semiconductor quantum well lasers. The model, based on Kane's two band theory, solves for the anisotropy in the constant energy surfaces and for the strong nonparabolicity of the bands. The system investigated is the EuSe–$PbSe_{0.78}Te_{0.22}$ quantum well structure at 77 K. The effects of nonparabolicity on the gain versus current-density relation are a reduction in the current density needed for any given gain and an increase in the gain saturation level. The nonparabolicity of the bands in the growth direction lowers the values of the confinement factor relative to parabolic bands which in turn lowers the modal gain values. Finally, the effects of nonparabolicity on the threshold current are significant for short cavity lasers and decrease with an increase in the cavity length.

I. INTRODUCTION

Quantum well structures have exhibited significant utility in the fabrication of advanced laser devices. Consequently, theoretical gain and current-density calculations have been performed to help understand the optoelectronic properties of these semiconductor microstructures.[1–7] Most of these calculations considered III–V semiconductor quantum well structures due to the availability of experimental data and the commercial importance of III–V lasers. Recently, IV–VI (also known as lead salt) quantum well heterostructures which exhibit strong quantum optical effects, have been used to fabricate mid-infrared diode lasers with greatly improved operating temperatures. Among the IV–VI compounds, single- or multiple-quantum well diode lasers have so far been fabricated in the PbEuSeTe–PbTe, PbSnTe–PbSeTe, and PbEuSe–PbSe material systems. At present, the PbEuSeTe quantum well system attained cw operation (at a 4.4 μm wavelength) up to 175 K, and pulsed operation (at 3.9 μm) up to 270 K.[8] The experimental and theoretical results to date suggest that for wavelengths of about 3–30 μm, lead salt lasers will operate at significantly higher temperatures than those from other materials.[8] In mid-infrared and far-infrared regions, these structures may play a key role in IR spectroscopy applications such as air pollution monitoring and IR integrated optics and IR telecommunication devices.[8]

These important applications are driving the need for a better understanding of IV–VI quantum well lasers. Therefore it is essential to perform theoretical gain and current-density calculations for the design and optimization of these important semiconductor quantum well laser systems. To establish a gain versus current-density model for the IV–VI semiconductor quantum well lasers, proper modifications to the III–V gain versus current-density formulation which are based on the constant spherical energy surface and a constant effective mass in all directions are needed. This paper discusses the effects of modifying the III–V model to incorporate anisotropic and nonparabolic band-structure characteristics of IV–VI semiconductors.

II. THEORETICAL MODEL

The system of interest in this work is shown in Fig. 1. The well material is $PbSe_{0.78}Te_{0.22}$[9] and the barrier material is EuSe with 77 K band gaps of 0.2 and 1.8 eV, respectively. This lattice matched structure is of interest because it is also lattice matched with BaF_2, a promising buffer material for growth of IV–VI semiconductors on silicon substrates.[10] The well growth is in the [100] direction and it is assumed that the discontinuities in the conduction-band and valence-band edges are equal. This assumption is valid based upon work by Partin[8] and Yuan *et al.*[11]

Using Kane's two band model, which is ideal in this case because it ignores the other four far bands, we solve for the anisotropy of the constant energy surfaces through calculations of the mobility effective masses in the conduction and valence bands for motion perpendicular and parallel to the substrate. The value of the mobility effective mass, in the well direction, at the band extrema (m_w^*) is calculated from the respective carrier longitudinal (m_l^*) and transverse masses (m_t^*) using the following equation[8]

$$\frac{1}{m_w^*}=\frac{1}{3}\left(\frac{2}{m_t^*}+\frac{1}{m_l^*}\right)=\frac{1}{m_{100}^*}. \tag{1}$$

The mobility effective mass in the conduction and valence bands are found equal to 0.05× the electron free mass. The same value is found for the carriers effective mass in the parallel plane to the substrate because of the equivalence ⟨100⟩ directions. The effects of nonparabolicity in the well bands on the gain versus injected carrier concentration and gain versus current-density relationships are investigated by dividing the study into four separate cases as shown in Table I.

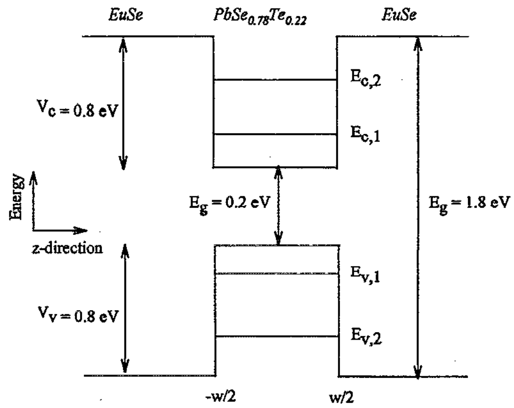

FIG. 1. EuSe–$PbSe_{0.78}Te_{0.22}$–EuSe quantum well structure at 77 K.

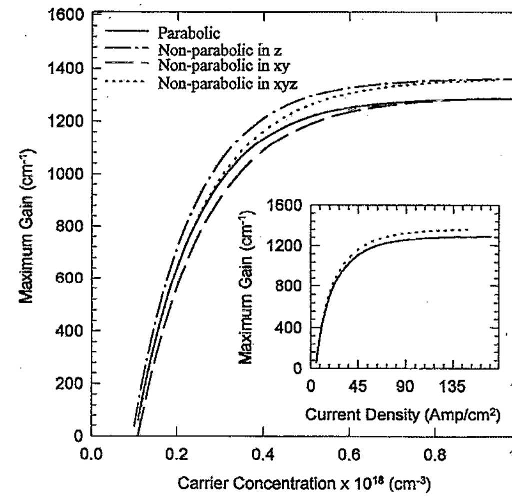

FIG. 2. Maximum gain as a function of carrier concentration for a 100 Å $PbSe_{0.78}Te_{0.22}$ quantum well system at 77 K. The four curves represent the four different cases explained in Table I. The inset is the maximum gain as a function of current density.

The gain calculations for the nonparabolic system are done using the following analytical form for the gain, which is used with parabolic system calculations where the intraband-relaxation processes are ignored[1–3]

$$\gamma(\omega_0)=\frac{\pi e^2\hbar\rho_{\rm red}}{\epsilon_0 n_{r,w} c m_0^2 w}\,\frac{|M_{{\rm QW},n}|^2_{\rm avg}}{\hbar\omega_0}\times[f_c(\omega_0)-f_v(\omega_0)]\sum_{n=1}^{\infty} H(\omega_0-\omega_n). \tag{2}$$

In Eq. (2), c is the speed of light, $n_{r,w}$ the index of refraction at the lasing frequency ω_0, ϵ_0 the permittivity of free space, m_0 the electron free space mass, w the well width, $(f_c\, f_v)$ the electron Fermi functions in the conduction and valence bands, $H(\omega_0-\omega_n)$ the Heaviside function, n the nth subband, and $\rho_{\rm red}$ the reduced density of states. $|M_{{\rm QW},n}|^2_{\rm avg}$ is the momentum matrix element in quantum well lasers for the TE mode:[2–4]

$$|M_{{\rm QW},n}|^2_{\rm avg}=\frac{3\xi}{4}\, m_0 E_g(1+\epsilon_n/E_c), \tag{3}$$

where ξ is a parameter that depends on the well material only. For IV–VI semiconductors, this parameter is related to the longitudinal mass, transverse mass, and the number of valleys (equal to four) via the following equation:[12]

$$\xi=\frac{4}{6}\left(\frac{m_0}{m_l^*}+\frac{2m_0}{m_t^*}\right). \tag{4}$$

The radiative component of the carrier recombination is found from the spontaneous emission rate[13]

TABLE I. The four cases studied in this work represent different assumptions regarding band parabolicity in the well-growth direction (z direction) and in the parallel plane to the substrate (xy plane).

Case	z direction	xy direction
1	parabolic	parabolic
2	nonparabolic	parabolic
3	parabolic	nonparabolic
4	nonparabolic	nonparabolic

$$R_{\rm sp}(\hbar\omega_0)=\frac{e^2 n_{r,w}\hbar\omega_0\rho_{\rm red}}{\pi m_0^2\epsilon_0\hbar^2 c^3 w}\,|M_{\rm conv}|^2_{\rm avg} f_c(\omega_0)\times[1-f_v(\omega_0)]\sum_{n=1}^{\infty} H(\omega_0-\omega_n). \tag{5}$$

Ignoring the nonradiative recombination, i.e., assuming a unity internal quantum efficiency value, the radiative current density is calculated from[13]

$$J=ew\int R_{\rm sp}(\hbar\omega_0)d(\hbar\omega_0). \tag{6}$$

III. RESULTS AND DISCUSSION

The gain calculations, assuming parabolic bands, are done following the analytical expression given in Eq. (2). The discrete energy levels in the well are calculated using the well-known square-well potential model. The gain values at the lasing frequency ω_0, or the maximum gain values, as a function of carrier concentration are plotted as solid lines in Fig. 2 for $w=100$ Å. The inset in the figure shows the maximum gain versus current density for the parabolic system. These two gain relations are typical for parabolic systems.[2–5]

Next we consider the effect of nonparabolicity on the gain calculations. First, we study nonparabolicity in the well-growth direction (z-direction). The discrete energy levels in the well can be calculated using either the Luttinger–Kohn equation or the energy dependent effective-mass method. For the structure under study, the difference in the bound states using these methods is small. Because of this small difference and to simplify the calculation procedure, the latter method is used to study the effects of nonparabolicity in the z direction on the gain versus current-density relation. The nonparabolicity in the well-growth direction shifts the bound-state energy levels calculated for the parabolic bands from 0.033 to 0.027 eV for the ground state.

The gain and current-density calculations, assuming nonparabolicity in the well-growth direction only, are done using the same gain expression given in Eq. (2) and current-density expression given in Eq. (6) where the parabolic energy levels are replaced by the nonparabolic energy levels. Figure 2 shows the results of gain calculations as a function of carrier concentration for the 100 Å well. The reduction of the bound-state energy due to nonparabolicity in the z direction shifts the gain versus carrier-density curve to the left of the parabolic curve. As a result, lower carrier densities are required to place the quasi-Fermi level above the quantized energy level and achieve the same gain as in the parabolic band case. In addition, the gain at a fixed carrier density is greater for the nonparabolic case due to the decrease in the photon energy at lasing.

Nonparabolicity of the bands in the perpendicular direction to the well-growth direction (xy plane) results in an energy dependent effective mass which in turn results in an energy dependent 2D density of states. The energy dependence of the density of states affects the gain and current-density calculations explicitly through ρ_{red} in Eqs. (2) and (6) and implicitly through the Fermi-level calculations. The Fermi-level calculations in the conduction and valence band required solutions for the first-order Fermi–Dirac integrals. In order to simplify these calculations we considered only the ground state in the well and disregarded the excited states. The maximum gain as a function of carrier concentration is plotted in Fig. 2 for the 100 Å well The nonparabolicity in the xy plane shifts the gain-carrier density curve to the right of the parabolic line because the energy dependent density of states requires higher carrier densities to achieve the same gain values as the parabolic case. The lowering of the nonparabolic gain curve with respect to the reference curve is due to the difference in the values of the Fermi functions (Fig. 2). One notices from Fig. 2 that the deviation of the nonparabolic z curve from the reference increases with carrier concentration. On the other hand, the deviation between the parabolic curve and the nonparabolic xy curve decreases with higher carrier concentration. This is due to the difference in the cause of the shift between the two cases.

Nonparabolicity in the well-growth direction and in the junction plane is referred to as nonparabolicity in the xyz directions. The effect of nonparabolicity on the gain versus carrier density curve increases with carrier concentration. At high carrier concentrations, the effect of nonparabolicity in the z direction dominates that of the nonparabolicity in the xy plane, while at low carrier concentrations the two effects approximately cancel. The radiative current density is calculated by integrating the spontaneous emission rate over the photon energy. Maximum gain versus current density for the parabolic approximation and for the nonparabolic bands in xyz is shown in the inset of Fig. 2. The effects of nonparabolicity include a reduction in the current density needed for any given gain and an increase in the gain saturation level.

The modal gain, determined by the optical confinement factor and the ability to collect injected carriers efficiently, is important in determining the quantum well optical properties.[13] To increase the effective active volume of quantum well lasers, multiple-quantum wells (MQW) and/or the

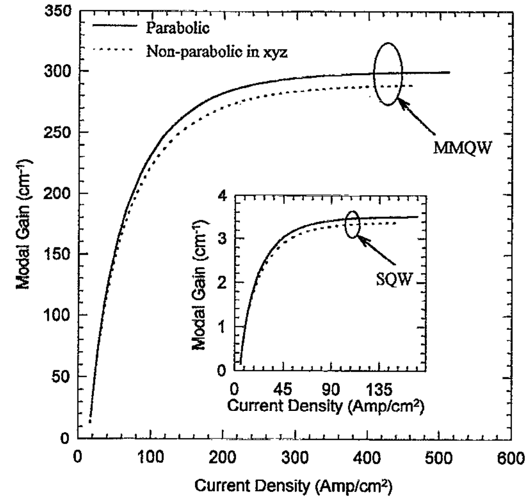

FIG. 3. The modal gain as a function of current density for three 100 Å $PbSe_{0.78}Te_{0.22}$ quantum wells at 77 K. The inset is the modal gain as a function of current density for a $PbSe_{0.78}Te_{0.22}$ SQW structure.

separate confinement heterostructure schemes[13] have been employed. In this study, modified multiple-quantum well (MMQW) structure consisting of a BaF_2/EuSe/$PbSe_{0.78}Te_{0.22}$/EuSe/BaF_2 lattice matched structure, where the well width is 100 Å, the barrier width is 25 Å, and the number of wells is three, is used. In order to obtain good uniformity of carrier concentration and maintain the two-dimensional properties of the well, the energy broadening for the ground state is kept at a value less than or equal to 1 meV.[2,3] By solving the Kronig–Penny model for both the parabolic and nonparabolic bands, a 25 Å barrier width is sufficient to satisfy the above energy broadening condition.

The results for modal gain versus current-density calculations for the MMQW structure are shown in Fig. 3. The MMQW curve shows a considerable increase in the modal gain as compared to the SQW structure because of increased optical confinement in the active region. The effects of nonparabolicity on the modal gain versus current density is similar to that of the SQW structure. The modal gain current-density curves for the SQW have an entirely different behavior from the maximum gain versus current-density curves shown in the inset of Fig. 2. This is an important result. The drop in the modal gain caused by nonparabolicity is due to the decrease in the optical confinement factor as a result of a shift in the photon lasing energy to a lower value. Detailed calculations on the effects of nonparabolicity on the confinement factor, modal gain, and threshold current will be presented and discussed in a future publication.

Because of the high modal gain values for the MMQW structure, we studied the effects of nonparabolicity on the threshold current for this particular structure. Threshold current calculations were performed assuming the width of the structure, which is mostly EuSe, has a constant value of 1 μm, while the cavity length L and the mirror reflectivities are variable parameters. Using the data of Fig. 3 and the laser oscillation condition, where the total losses in the waveguide are equal to the modal gain value at the lasing frequency, the

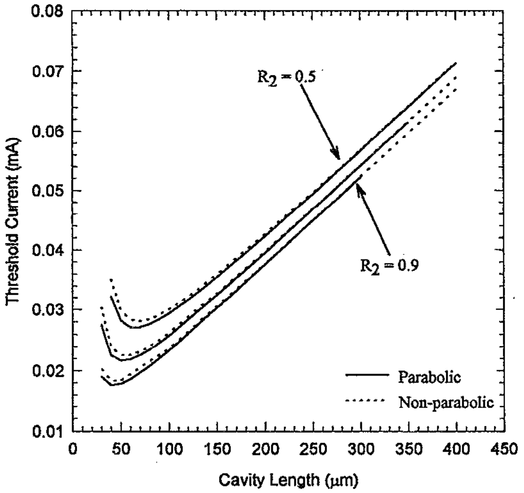

FIG. 4. Threshold current vs cavity length for the $PbSe_{0.78}Te_{0.22}$ MMQW structure with R_2 as a parameter and R_1 fixed at 0.9.

threshold current-cavity length relation for the MMQW structure is calculated and shown in Fig. 4. The reflectivity at one end, R_1, is fixed at 0.9 and the reflectivity at the other end, R_2, is chosen to be 0.5, 0.7, and 0.9. From these plots, one notices that increasing the reflectivity of one of the ends decreases the threshold current values as expected. Moreover, each curve has a minimum threshold current value at a critical cavity length. The region above the critical length corresponds to the low modal gain regime (or low losses regime) where $I_{th} \propto L$. However, the region below the critical cavity length value corresponds to the high modal gain regime (or high losses regime) where the modal gain increases more slowly with the current density than at lower values of the modal gain.

The effects of nonparabolicity are more noticeable in the high gain regime (or high loss regime) than in the low gain regime (or low loss regime); see Fig. 3. Therefore, for a fixed total loss value in the low loss regime, the effects of nonparabolicity on the threshold current are very small. Increasing the total loss by decreasing L or R_1R_2, these effects become more pronounced as shown in Fig. 4. For a mid-infrared laser, where the cavity length is typically greater than 250 μm, the effects of nonparabolicity on the threshold current can be neglected without loss of accuracy. However, these effects are significant for short cavity lasers and must be considered, for example, when designing vertical surface-emitting lasers (VCSELs). The effects of nonparabolicity on very short lasers such as VCSELs are left for future work.

IV. CONCLUSION

In conclusion, a theoretical model that calculates the gain versus current-density relation for IV–VI semiconductor quantum well lasers has been developed. The theory is based on Kane's two band model. The effect of nonparabolicity of the bands in the growth direction is to shift the quantized energy levels toward the band edge while nonparabolicity in the substrate plane results in an energy dependent reduced density of states. The impact of nonparabolicity on the gain versus carrier density relation increases with carrier concentration. At high carrier concentrations, the effects of nonparabolicity in the growth direction dominate the effects of nonparabolicity in the substrate plane, while at low carrier concentrations the two effects approximately cancel. The effect of nonparabolicity in all directions on the gain versus current-density relation is a reduction in the current density needed for any given gain and an increase in the gain saturation level. The nonparabolicity of the bands in the growth direction lowers the values of the confinement factor relative to those for the parabolic bands which in turn lowers the modal gain values. In addition to the 20% shift in the output lasing energy, the effects of nonparabolicity on the threshold current values are negligible for long cavity lasers.

Finally, more careful treatment of the related physical processes and material parameters, namely, inclusion of the intraband-relaxation process and the nonradiative current components due to the leakage current out of the active region and to the Auger process, is needed. In this work, the effects of nonradiative current components in the above model are believed to be small because of the barrier height (0.8 eV) which reduces the leakage current and the low temperature used in this study (77 K) which reduces the effects of Auger processes. Moreover, theoretical and experimental data from a detailed study, performed by Nagarajan *et al.*,[7] on MQW GaAs/AlGaAs quantum well lasers showed that the radiative current component proportionally increases with the number of wells and all nonradiative current components become small except at very short cavities.

[1] Y. Arakawa and A. Yariv, IEEE J Quantum Electron. **21**, 1666 (1985).
[2] Y. Arakawa and A. Yariv, IEEE J. Quantum Electron. **22**, 1887 (1986).
[3] M. Asada, A. Kameyamaan, and Y. Suematsu, IEEE J. Quantum Electron. **20**, 745 (1984).
[4] N. K. Dutta, J. Appl. Phys. **53**, 7211 (1982).
[5] D. Kasemset, C. Hong, N. B. Patel, and D. Dapukus, IEEE J. Quantum Electron. **19**, 1025 (1983).
[6] A. Sugimura, IEEE J. Quantum Electron. **19**, 932 (1983).
[7] R. Nagarajan, T. Kamiya, and A. Kurobe, IEEE J. Quantum Electron. **25**, 1161 (1989).
[8] D. L. Partin, IEEE J. Quantum Electron. **24**, 1716 (1988).
[9] P. J. McCann and C. G. Fonstad, Thin Solid Films **227**, 189 (1993).
[10] H. Zogg, Appl. Phys. Lett. **49**, 993 (1986).
[11] S. Yuan, H. Krenn, G. Springholz, and G. Bauer, Appl. Phys. Lett. **62**, 885 (1993).
[12] P. K. Cheo, *Handbook of Solid-State Lasers* (Dekker, New York, 1989).
[13] S. Chinn, Appl. Opt. **23**, 3508 (1984).